Author Manuscript

Author Manuscript

Author Manuscript

Author Manuscript

HHS Public Access

Author manuscript

Exp Neurol. Author manuscript; available in PMC 2018 November 01.

Published in final edited form as:

Exp Neurol. 2017 November ; 297: 179–189. doi:10.1016/j.expneurol.2017.08.004.

Motor cortex and spinal cord neuromodulation promote corticospinal tract axonal outgrowth and motor recovery after cervical contusion spinal cord injury

N. Zareen[a], **M. Shinozaki**[a,1,2], **D. Ryan**[a], **H. Alexander**[a], **A. Amer**[a,b], **D.Q. Truong**[c], **N. Khadka**[c], **A. Sarkar**[a], **S. Naeem**[a], **M. Bikson**[c], and **J.H. Martin**[a,b,*]

[a]Department of Molecular, Cellular, and Biomedical Sciences, City University of NY School of Medicine, New York, NY 10031, USA

[b]CUNY Graduate Center, New York, NY 10031, USA

[c]Department of Biomedical Engineering, City College of NY, 10031, USA

Abstract

Cervical injuries are the most common form of SCI. In this study, we used a neuromodulatory approach to promote skilled movement recovery and repair of the corticospinal tract (CST) after a moderately severe C4 midline contusion in adult rats. We used bilateral epidural intermittent theta burst (iTBS) electrical stimulation of motor cortex to promote CST axonal sprouting and cathodal trans-spinal direct current stimulation (tsDCS) to enhance spinal cord activation to motor cortex stimulation after injury. We used Finite Element Method (FEM) modeling to direct tsDCS to the cervical enlargement. Combined iTBS-tsDCS was delivered for 30 min daily for 10 days. We compared the effect of stimulation on performance in the horizontal ladder and the Irvine Beattie and Bresnahan forepaw manipulation tasks and CST axonal sprouting in injury-only and injury + stimulation animals. The contusion eliminated the dorsal CST in all animals. tsDCS significantly enhanced motor cortex evoked responses after C4 injury. Using this combined spinal-M1 neuromodulatory approach, we found significant recovery of skilled locomotion and forepaw manipulation skills compared with injury-only controls. The spared CST axons caudal to the lesion in both animal groups derived mostly from lateral CST axons that populated the contralateral intermediate zone. Stimulation enhanced injury-dependent CST axonal outgrowth

*Corresponding author at: Department of Molecular, Cellular, and Medical Sciences, City University of NY School of Medicine, 160 Convent Avenue, New York, NY 10031, USA. jmartin@ccny.cuny.edu (J.H. Martin).

[1]Permanent address: Department of Physiology, Keio University School of Medicine, Shinjuku-ku, Tokyo 1608582, Japan.

[2]Co-first authors.

Author contributions

MS, NZ, and JM designed the experiments and wrote and edited the manuscript

MS and NZ performed the C4 contusions, CST tracings, and all other surgical procedures, as well as performed the daily tsDCS and iTBS stimulation

AA and JM designed the 10 day contusion tsDCS neuromodulation of M1-evoked EMG experiment and AA recorded and analyzed the data

DR and HA performed the behavior training in animals

DR, HA, and SN performed behavioral analyses

MS, HA, AS, and JM analyzed CST data

DT and MB designed the FEM modeling experiments and constructed the images

AS performed tissue compartment segmentation

NK and JM designed the CST imaging protocol and NK wrote the Matlab scripts and performed the analyses

Author Manuscript Author Manuscript Author Manuscript Author Manuscript

below and above the level of the injury. This dual neuromodulatory approach produced partial recovery of skilled motor behaviors that normally require integration of posture, upper limb sensory information, and intent for performance. We propose that the motor systems use these new CST projections to control movements better after injury.

Keywords

Intermittent theta burst stimulation; Trans-spinal direct current stimulation; FEM modeling; Corticospinal tract; Motor cortex; Cervical contusion; Skilled limb movement; Rat

1. Introduction

Cervical injuries are the most common form of SCI (NSCISC, 2014). People with a cervical injury value hand use as their highest priority for recovery (Anderson, 2004). There is a pressing need for effective therapies for promoting the function of the injured cervical spinal cord and restoring upper extremity use. The motor signs after SCI are due to interruption of descending control signals from the brain and the major source of these signals arise from the motor cortex (M1). Indeed, the loss of voluntary and skillful arm control is largely attributable to the loss of corticospinal tract (CST) control of cervical motor circuits. To restore this control requires reconnecting the damaged CST with the spinal cord below the injury. This is a daunting task, despite the many new directions for neural repair (Benowitz et al., 2017; Park et al., 2010).

Most SCIs are incomplete (Chen et al., 2016), offering the opportunity to foster reconnecting the brain with the spinal cord below the lesion by sprouting of spared CST axon. An effective strategy to restore function after a pyramidal tract lesion is to promote CST sprouting into the denervated side (Carmel et al., 2010; Maier et al., 2008). We have developed a neural activity-based approach in which M1, the principal source of the CST, is electrically stimulated (Brus-Ramer et al., 2007). Previously, we demonstrated that M1 epidural stimulation (which we term multi-pulse stimulation, or MPS) 6 h a day for 10 days promotes ipsilateral CST sprouting in naïve animals and, importantly, into the denervated side of the spinal cord after a pyramidal tract lesion. This stimulation therapy fully restored skilled locomotion after pyramidal tract lesion, when applied immediately after the lesion (Carmel et al., 2010) or delayed by 7 weeks (Carmel et al., 2014). By contrast, animals with injury-only do not show any recovery.

The logic of this neuromodulatory strategy derives from our developmental studies showing the importance of activity in steering normal development of the CST (Friel and Martin, 2007; Martin et al., 1999). Postnatal stimulation of the CST—at currents producing muscle activation (Salimi et al., 2008; Salimi and Martin, 2004), in order to ensure activation of spinal cord targets—helped establish spinal connections. This stimulation-based strategy is challenged after serious SCI because few axons remain caudal to the injury to activate damaged spinal motor circuits. Indeed, after SCI or brain injuries that interrupt the CST, the thresholds for evoking motor responses increase substantially and response onset is delayed (for review, see (Oudega and Perez, 2012)).

Author Manuscript Author Manuscript Author Manuscript Author Manuscript

In this study, we used a moderate C4 bilateral contusion model to interrupt CST projections to the cervical enlargement with minimal forelimb motoneuron involvement. This contusion produces a large central lesion that spares few axons in the rat (Anderson et al., 2009). We chose this model because it closely approximates the pathology of SCI in humans (Anderson et al., 2005; Sharif-Alhoseini et al., 2017) and it represents a highly demanding standard that must be achieved in order to move forward with a therapy. To facilitate the actions of the CST on damaged spinal motor circuits after SCI we used cathodal trans-spinal direct current stimulation (tsDCS). In contrast to transcranial direct current stimulation, where anodal stimulation is facilitatory, cathodal stimulation strongly enhances M1-evoked response in the intact spinal cord (Song et al., 2015), possibly by facilitating ventral spinal circuits (Song and Martin, 2017). For M1 electrical stimulation, we used an intermittent theta burst stimulation protocol (iTBS). In our recent study (Song et al., 2016), iTBS with cathodal tsDCS 30 min daily for 10 days was as effective as MPS in achieving significant CST outgrowth and functional improvement after pyramidal track lesion. iTBS has the added benefit of requiring a shorter daily stimulation period than MPS and could thus be a more translational neuromodulatory stimulus. Further, since SCIs are not strongly lateralized we electrically stimulated M1 bilaterally.

We studied the effect of combined tsDCS and iTBS, delivered 30 min daily for 10 days, on CST axonal sprouting and recovery of motor function. We examined performance in the horizontal ladder task (Metz and Whishaw, 2002) and the Irvine, Beattie and Bresnahan forepaw manipulation task (Irvine et al., 2010; Irvine et al., 2014), both of which display a strong dependence on corticospinal control. We used Finite Element Method (FEM) modeling to position the tsDCS electrodes in order to maximize the density of applied currents in the cervical enlargement and, in turn, the potential for facilitatory neuromodulation of cervical motor circuits (Song et al., 2015). We show that this combined spinal-M1 neuromodulatory approach significantly promotes recovery of skilled locomotion and forepaw manipulation skills and enhances injury-dependent CST axonal outgrowth below and above the level of the injury. Our findings show that a short period of daily M1 stimulation, together with tsDCS to augment M1-evoked motor responses, is an effective neuromodulatory approach to promote forelimb skilled functions after cervical SCI. We propose that the motor systems use these new CST projections to control movements better after injury.

2. Methods

Thirty-two adult female Sprague-Dawley rats (250 to ~300 g) were used in this study (for the chronic study: 14 injury-only; 13, injury plus stimulation; for acute electrophysiology: 3 injury-only; for computer modeling: n = 2, injury only). Experiments were approved by the Institutional Animal Care and Use Committee of the City College of New York and the CUNY Advanced Science Research Center. All CST and behavioral analyses were conducted by laboratory personnel blinded to the animal's condition (injury-only versus injury plus stimulation). For the injury plus stimulation condition, motor cortex stimulating electrodes were implanted 2–3 weeks before the animals were trained in the horizontal ladder and IBB behavioral assessment (Fig. 1A; see below). Injury-only animals did not receive electrode implantation.

Author Manuscript Author Manuscript Author Manuscript Author Manuscript

2.1. Bilateral M1 electrode implantation

Animals were anesthetized using a mixture of Ketamine (90 mg/kg) -Xylazine (10 mg/kg). Animals were placed in a stereotaxic frame and a craniotomy was made bilaterally over the left and right M1 to expose the forelimb representations. We used the same cortical epidural stimulating electrode as in our earlier studies (PlasticsOne, Inc.; e.g., (Brus-Ramer et al., 2007)). Bilateral electrodes were placed over the M1 forelimb areas epidurally (with respect to bregma: AP 1.5–2.0; ML ± 3–3.5). We verified that the electrode evoked a contralateral forelimb movement (or muscle contraction) and not ipsilateral forelimb movements or hind limb movements, indicating correct placement over the M1 forelimb representation.

2.2. C4 laminectomy and contusion

We performed a C4 midline contusion. A midline incision was made from T2 to the base of the skull and the dorsal neck muscles bluntly dissected to expose the cervical vertebrae from C2 to T2. A laminectomy was performed at C4 sufficiently large so that the impactor probe cleared the bone margins. The rats were suspended on the stabilization platform of the Infinite Horizon (IH) spinal impactor. The spinal cord was held in a level position without any twists. The lateral edges of the vertebral bodies at C3 and C5 were grasped with the fixation forceps of the impactor to stabilize the cord for impact. The impact probe (3.5 mm diameter; tip configuration; inset Fig. 1B) was lowered to the dura at C4. A dissecting microscope was used at 200 × magnification to verify that the probe was positioned correctly at the C4 midline. Stability of the vertebral column was verified by gently tapping the C4 vertebra. The probe was raised 3.9 mm (3 turns on the Infinite Horizon impactor elevation dial) before initiating the hit. We produced a 200 kdyn impact with zero dwell time. After surgery, animals were returned to a holding cage that was set on a heating pad, and observed until ambulatory. An analgesic (Carprofen; 4 mg/kg) and antibiotic (Baytril; 5 mg/kg) were administered.

2.3. Lesion confirmation

During the contusion procedure we verified that the probe was not impeded by bone or other tissues during impact. A small petechial hemorrhage and bruising parallel to the midline were evident at the impact site. Postmortem histological assessments were made using Hematoxylin and Eosin (H & E) staining in all animals. To measure lesion volume, the section of maximal lesion area and adjoining rostral and caudal sections were chosen for analysis. Using Neurolucida (MBF Bioscience), a contour of the lesion was drawn, as well as a contour of the entire section. Neurolucida Explorer was used to compute the average lesion area for each animal. We constructed a lesion overlap image for each animal group (see Fig. 1C, E).

2.4. iTBS and tsDCS

An epidural electrode was used to deliver the phasic iTBS electrical stimulation (Fig. 1F). The stimulation pattern was the same as in our previous study (Song et al., 2016). The electrical iTBS consists of delivering a burst of 3 pulses (interstimulus interval: 50 ms), repeated 10 times, for 2 s followed by 8 s without stimulation; this was repeated 20 times, for a total of 600 pulses. In our previous study, we systematically evaluated stimulation

Author Manuscript Author Manuscript Author Manuscript Author Manuscript

parameters. Over a range from 3 to 100 ms, 50 ms produced the strongest facilitation. The basic electrical iTBS protocol was based upon the published TMS protocol of Huang and colleagues (Huang et al., 2005). This comprised the basic iTBS stimulation block. The iTBS block was repeated 5 times. The reason for using multiple iTBS blocks is based on rat TMS studies (Benali et al., 2011), which show downregulation of parvalbumin-positive inhibitory interneurons in the stimulated rat MCX, suggesting disinhibition as a mechanism. The stimulation intensity for iTBS was chosen as 75% of motor threshold level, defined as the intensity of a stimulus (330 Hz; 45 ms duration, for a total of 14 pulses) to evoke a movement in response to ~50% of the stimuli presented.

tsDCS was produced through hydrogel electrodes on the skin surface (see Fig. 2; StimTent Com; 0.5″ × 1.5″). The current was set at −1.5 mA (3 × 10ˆ−3 mA/mmˆ2). Current was ramped from zero to 1.5 mA over 2.5 s and returned to zero over 2.5 s. The cathode was placed over the C4-T2 vertebrae and the anode, over the chest (see Fig. 2). We used Finite Element Method (FEM) modeling to predict that this electrode configuration induces maximal current density within the cervical enlargement (see Results section). Rats were stimulated in their home cage and showed no signs of distress during experiments. iTBS and tsDCS were delivered using the programmable waveform/pulse generator (A-M Systems, model 3800) and stimulus isolation units (A-M Systems, model 3820).

2.5. Ladder training and analysis

Rats were trained to walk along a horizontal ladder (Carmel et al., 2010; Metz and Whishaw, 2002), from one side to the other without stopping, until their forelimb error rate was approximately 10%. Over the course of two weeks, rats were trained to perform the task. Animals were first accustomed to the task apparatus and then trained to walk across a horizontal ladder without gaps between rungs. Next, every other rung was removed from the ladder, and the rat learned to step over the resulting gaps. Finally, the spacing of the ladder rungs was made irregular, with gaps ranging from one to two rungs. The rung pattern was changed after every 12 runs to prevent the rats from memorizing a specific pattern. This stage of training usually ranged from 3 to 4 days. After training was completed, a baseline score was calculated for the rat by videotaping 24 runs back and forth across the ladder (Sony Handycam FDR-AX33 Digital Camcorder). The error rate was calculated by watching the recorded runs in slow motion and determining whether the paw placement on the ladder rungs for each step was normal, too far forward with the digits not grasping the rung (overstep), too far back with the wrist below the rung and grasping by the digits (understep), or missing the rung entirely (miss). The percent error was calculated by adding up the total number of oversteps, understeps, and misses for each forelimb and dividing by the total number of steps taken using that forelimb. The values for the left and right forelimbs were computed separately and added together to determine the total error rate. The videos were scored blinded.

The percentage of errors within a session was used as the behavioral performance outcome measure. Performance typically was assessed within 5 days before lesion (baseline) and then 3 weeks after injury without additional training in between. Animals were then tested once a

Author Manuscript Author Manuscript Author Manuscript Author Manuscript

week for 4 weeks. The low frequency of testing after injury made it unlikely that the animals derived therapeutic benefit from these sessions.

2.6. IBB training and analysis

The Irvine, Beattie, and Bresnahan forepaw manipulation score (Irvine et al., 2014) was used to compare changes in distal motor skill produced by injury alone and injury plus stimulation. Animals were acclimated to the food for manipulation and eating by providing pieces of spherical and donut shaped cereal in their home cage for several days before testing. Rats were accustomed to the testing environment, which was a plastic cylinder, for 10–15 min daily for 2–3 days. Animals were tested at baseline, before injury, and at weeks 4 and 6 post-injury. During testing sessions, animals were placed into the cylindrical testing environment. Four to five pieces of cereal were placed in the cylinder and the rats were allowed to eat the cereal. Forepaw movements used to manipulate and eat the food were videotaped.

The videos were scored blinded using the published guidelines for reliability and validity (Irvine et al., 2014). In each of these videos, nine different categories were scored according to the published scoring sheet (Irvine et al., 2014): 1) predominant elbow joint position; 2) proximal forelimb movements; 3) contact with non-volar support; 4) predominant forepaw position; 5) contact with volar support; 6) cereal adjustments; 7) wrist movement; 8) presence of digit movements; 9) grasping method. Each of the 9 categories is observed hierarchically when analyzing the videos. Using the published score sheet, for the right and left forelimbs while consuming spherical and donut shaped cereal, a final score was determined according the published criteria. The scores for spherical and donut cereal for each side were averaged together to obtain a final score for each forelimb. The total score was the average of all four scores. The maximal score is 9.

2.7. Motor evoked potentials and analysis of animals with C4 contusion

We determined the effect of C4 contusion on motor threshold (minimal current to evoke a contralateral forelimb movement) and the effect of cathodal tsDCS. In a separate group of animal, M1 epidural stimulating electrodes (Plastics One) were implanted bilaterally over the forelimb area, as described above for chronic stimulation. After recovery, animals were tested under light Ketamine anesthesia (90 mg/kg IP) before C4 contusion (as described above) and once between day 10–20 after the injury. Animals in the injury plus stimulation group received therapeutic stimulation during this time period.

2.8. Protocol for daily therapeutic stimulation

Sutures were removed 3 to 4 days before onset of the stimulation period to allow the skin to heal. Depilating lotion (Nair or Veet) was used to remove fur from the dorsal and ventral tsDCS stimulation sites the day before the onset of stimulation. Animals were connected to the iTBS stimulator using a swivel commutator (PlasticsOne). The contralateral forepaw movement thresholds for each forelimb was determined using the 14 pulse stimulation paradigm described above. Currents used for chronic iTBS stimulation were chosen to be at approximately 75% of the current thresholds for the 14 pulse stimulation. tsDCS electrodes were placed over the skin, targeting the cervical enlargement (location estimate based on

Author Manuscript Author Manuscript Author Manuscript Author Manuscript

FEM modeling, see Fig. 2) (Song et al., 2015) and secured by placing the animal in a rodent jacket (Braintree Scientific).

2.9. GST tracing

After completion of the last behavioral testing session, rats were anesthetized and placed in a stereotaxic frame and body temperature was maintained at 37 °C by a heating blanket. The epidural electrode implant was removed to expose the dura over M1, a procedure that does not produce M1 trauma (Carmel et al., 2010; Carmel et al., 2013). Seven pressure injections (300 nl/each) of biotinylated dextran amine (BDA; 10,000 MW; Molecular Probes; 10% in 0.1 M PBS) were made in the forelimb M1 (depth 1.5 mm, lateral 2.5 to 3.5 mm; rostral: 0.5 to 2.5 mm; separated by 0.5 mm each injection site). Two weeks later, rats were euthanized by an anesthetic overdose and transcardially perfused (300 ml saline followed by 500 ml 4% paraformaldehyde). Tissue containing the lesion site and cervical spinal cord were dissected, post-fixed in 4% paraformaldehyde for 2 h and transferred to 20% sucrose (overnight at 4 °C). Transverse sections of brain stem and spinal cord were cut (40 μm thickness). To visualize BDA-labeled CST axons, sections at C3 and C7 spinal segments were incubated in phosphate-buffered (pH 7.4) saline containing 1% avidin-biotin complex reagent (ABC kit; Vector Laboratories) and 0.2% Triton X-100 (Sigma), for 2 h at room temperature. After rinsing, sections were incubated with diaminobenzidine (Sigma) for 20 min. After rinsing again, sections were mounted on gelatin-coated slides, air-dried overnight, and cover slipped.

2.10. CST anatomical analysis

We assayed changes in CST axon length caudal and rostral to the injury. All CST measurements were conducted by laboratory personnel blinded to animal group. For CST projections caudal to the injury, essentially all gray matter labeling was located contralaterally. We therefore restricted our analysis to the contralateral side for measurements caudal to the injury as well as rostral, for consistency. To measure CST axon length caudal to the injury we used NeuroLucida (MBF Bioscience, Williston, Vermont USA). Since labeling on sections was sparse due to the injury, axon length was traced manually at C7 with the axon tracing tool at 400 × magnification. Axon varicosities (3 times adjoining axon diameter) were also measured using markers. Other studies have shown a strong association between varicosities and co-labeling with synaptic markers (Friel et al., 2012; Meng et al., 2004). We traced 6 sections per animal and obtained an average of axon length and varicosities. Spared axons in the white matter were manually counted in contralateral and ipsilateral lateral columns as well as in the ventral medial area.

Due to the high density of CST projections rostral to the injury at C3, we used an unbiased stereological estimate (Stereo Investigator; ‘Spaceball;’ MBF Bioscience, Williston, Vermont, USA), similar to our earlier studies (Carmel et al., 2010; Song et al., 2016). Briefly, the contralateral gray matter border was traced and the program divided the region into 50 μm by 50 μm squares. Within each measurement square a sampling sphere of 10 μm diameter (‘space ball’) was established by the program. Intersections between labeled axons and the sampling sphere were marked under 1000 × magnification. An intersection is defined as a contact or crossing of an axon with the cross-section of the sphere, and is saved

Author Manuscript Author Manuscript Author Manuscript Author Manuscript

as a single-pixel dot image. The number of intersections within each 50 μm square volume was used to estimate local axon length based on sphere volume and tissue thickness (Mouton et al., 2002).

As in a previous study (Carmel et al., 2010), we used the Optical Dissector (Stereo Investigator) under 1000 × magnification to estimate the number of labeled CST axons in the ventral dorsal column at C3. This was used to correct for tracer efficacy and for analyses estimating gray matter axon length per labeled CST white matter axon. Tracer efficacy did not differ between the injury-only and injury plus stimulation groups (Average DC axon counts injury-only = 2142; injury plus stimulation = 2357; $p = 0.48$). This is similar to our prior studies examining the effect of stimulation on pyramidal tract lesion sprouting (Brus-Ramer et al., 2007).

2.11. Heat map analyses

Color-coded maps (“heat maps”) of corrected regional CST axon length and varicosity density caudal to the injury were constructed using Matlab and registered with the gray matter border. Axon and varicosity measurements, made using Neurolucida, were exported as TIFF files of traced axons and single-pixel markers for a varicosity of individual sections. For rostral to the lesion, only CST axon length maps were constructed. Measurements were made using StereoInvestigator and exported as images of individual sections representing intersections as single pixels. All images were analyzed using customized Matlab scripts, where functions were defined to read images for each animal within a group and to perform a smoothing operation (customized isotropic Gaussian averaging and smoothing kernel with a standard deviation of 36 along all dimensions; ‘*imgaussfilt*’ Matlab function) to enhance the image quality by reducing high-frequency noise components and implement a factor based on CST axon counts to correct for tracer efficacy. This smoothing function determines the appropriate filter size based on the specified standard deviation to avoid filter truncation. In addition, this function allows for fine control of the amount of smoothing. After each image of each animal within the injury-only or injury + stimulation group was processed through the aforementioned smoothing function, all images were saved in an array. Finally, an average across all images was calculated to generate “mean-of-mean” average heat maps. When comparing axons or varicosities side-by-side, color scales are the same. Areas without labeling are plotted indigo.

2.12. Finite Element Method computational model to predict spinal regional current density during c-tsDCS

Finite Element Method (FEM) computational models of tissue current flow during electrical stimulation, based on anatomical scans (MRI, CT), are considered reliable predictors of electric field and current density within the brain and spinal cord (Hernandez-Labrado et al., 2011; Rahman et al., 2013; Toshev et al., 2014). As the model makes only basic assumptions on physics (i.e., Ohms law), the precision of model predictions is limited by the quality of tissue segmentation and assigned tissue conductivity (Toshev et al., 2014). We constructed our own FEM current density models of rat spinal cord (Song et al., 2015). We used MRI (7.0 Tesla 70/30 Bruker Biospec) with a TurboRARE T2-weighted pulse sequence to image soft tissues and microCT (Siemens Inveon) to image bone in two female rats with

Author Manuscript Author Manuscript Author Manuscript Author Manuscript

laminectomies and spine contusions at 10 and 12 days post-injury. MRI settings achieved a 0.234 mm resolution and microCT, 0.196 mm. MRI and CT images were co-registered to the CT image space using functions available in Statistical Parametric Mapping (SPM8, Wellcome Trust Centre for Neuroimaging, London, UK). Segmentation was completed semi-manually within ScanIP (Simpleware, Exeter, UK) with the aid of tools such as thresholding, threshold flood-filling, Gaussian smoothing, dilation, and erosion. Each slice of the MR image of the brain and spinal cord was carefully outlined. The dura was traced and the intervening space between the dura and brain or spinal cord comprised the CSF compartment. The lesion tissue in each animal was manually segmented as either fluid or blood based on the T2 data. All soft tissues (including skin, muscle, fat, tendons) comprised a single compartment. All bones were outlined from CT data.

The + FE module of ScanIP was then used to generate an adaptive volumetric mesh of approximately 6.8 million tetrahedral elements. Electrostatic physics were modeled in COMSOL (COMSOL Inc., Burlington, MA, USA) using the following boundary conditions: inward current density summing to 1 mA on the ventral surface anode electrode, ground on the dorsal surface cathode electrode, insulation on all other external surfaces, and continuity for internal boundaries. Results were linearly scaled to other stimulation intensities. Tissue conductivity for the model was assigned based on approximation from published values used in human simulation studies, which themselves are aggregates of animal data (Gabriel et al., 1996; Huang et al., 2017; Wagner et al., 2007). We used the following values (in Siemens/m): muscle, 0.16; bone, 0.01; cerebral spinal fluid (CSF), 1.65; gray matter, 0.276; white matter, 0.126; air, 1e-15; conductive gel or saline, 1.65; electrode, 5.99e7; blood, 0.67. The electrode position was accurately referenced to the dorsal spinous process at T1 or the posterior ridge of the occipital bone and the sternum, ventrally. The resulting finite element problem was solved for voltage and calculated current density. Results are presented both as current density on the reconstructed brain and spinal cord surfaces and within the spinal cord along the midsagittal axis.

2.13. Statistical analyses

We used the programs Prism (5.0) and Microsoft Excel to determine the statistical significance of differences between injury-only and injury plus stimulation groups. A two-sample Kolmogorov-Smirnov (K-S) test was used to compare the cumulative distribution datasets. Regression analyses were conducted using the program KaleidaGraph (version 4.5.3). The graphs plot the mean ± the standard error of the mean, unless otherwise specified. The significance level was set at 0.05.

3. Results

3.1. C4 contusion injury

Representative H & E-stained sections from injury-only (Fig. 1B) and injury plus stimulation (D) animals show the large central cavity, which is characteristic of contusion injuries in rats (Anderson et al., 2009; Scheff et al., 2003). There was no significant difference in lesion size in the two animal groups (Injury-only: 36.8% ± 2.8%; Injury plus Stimulation: 41.5% ± 3.7; unpaired *t*-test: p = 0.32). Lesion overlap images for each animal

Author Manuscript Author Manuscript Author Manuscript Author Manuscript

group (Fig. 1C, E; right) indicate that all animals sustained complete lesion of the dorsal CST. The lateral and ventral CST were partially spared in most animals.

3.2. FEM modeling to direct tsDCS

To determine the optimal placement of the tsDCS surface electrodes, we conducted FEM modeling in two rats with C4 injury to estimate DC current flow within the cervical spinal cord (Song et al., 2015). The cathode was placed dorsally and the anode, ventrally (Fig. 2C, inset). We modeled multiple electrode placements relative to the T1 vertebra, which has a prominent spinous process that can be palpated in the intact animal. Based on predictions of current density (data not shown), we chose the electrode placement that maximized current density in the region of the cervical enlargement (the configuration shown in Fig. 2). Whereas applied currents between the cathode and anode flow throughout the entire body by conduction through different tissues, (Fig. 2 inset), the highest density is in the cervical enlargement. These currents are represented on the dural surface (A–D) as well as in midline section (E, F) as a color scale. In summary, using FEM modeling we show that current can be preferentially directed to the cervical enlargement segments after injury, which is the most relevant portion of the cervical spinal cord for forelimb control.

3.3. tsDCS neuromodulation promotes M1-evoked muscle responses after SCI

After SCI, M1-evoked responses require higher stimulation amplitudes to be produced and the size of the responses are smaller than in normal individuals (for review, see (Oudega and Perez, 2012)). To increase the efficacy of M1 stimulation in activating spinal motor circuits we used cathodal tsDCS. This form of spinal DC neuromodulation preferentially enhances evoked ventral spinal cord responses (Song and Martin, 2017) and MEPs in intact animals (Song et al., 2016; Song et al., 2015). In a separate group of animals (n = 3) we conducted serial electrophysiological experiments to determine the changes in M1-evoked muscle responses after C4 contusion and the impact of cathodal tsDCS on M1 evoked responses in injured animals. These animals were instrumented with chronic M1 stimulating electrodes similar to the chronically stimulated animals. We used a standard electrical stimulation pattern (14 pulses, 333 Hz) to obtain the motor threshold, which was defined as the lowest current that consistently evoked a contralateral forelimb movement. At this current, we did not observe ipsilateral or hind limb movements indicating selectivity for forelimb M1. We observed a 60% increase in motor threshold 10 days after injury (before lesion: 2.1 mA ± 0.19 mA; after lesion: 3.3 mA ± 0.6 mA).

We next determined the capacity of cathodal tsDCS to enhance M1-evoked motor evoked potentials (MEP) after injury. We tested the effect of tsDCS using 3 pulses (333 Hz), which evokes a single MEP (Fig. 3A, B insets), at 75–85% (A) and 100% (B) of the threshold current. Cumulative histograms (Fig. 3A, B) indicate that MEPs were infrequent and small at both current levels without tsDCS neuromodulation; predictably smaller at 75–85% than 100% threshold. With tsDCS, there was a significant shift towards larger and more frequent responses, from 80% to 41% of stimuli failing to evoke a response for 75–85% threshold stimulation and from 55% to 12% of stimuli failing to evoke a response for 100% threshold (75–85%: $p < 0.001$; 100%: $p < 0.001$; Kolmogorov-Smirnoff test). Averaged EMG responses at both stimulus levels show approximately a 4-fold increase in the integrated

Author Manuscript Author Manuscript Author Manuscript Author Manuscript

EMG response (Fig. 3C) using cathodal tsDCS (75–85% threshold: 45.2 ± 6.2 versus 240 ± 32.2; p = 0.019; 100% threshold: 108.2 ± 8.5 versus 393.2 ± 25.6; p = 0.003). These electrophysiological assessments of MEPs show that tsDCS, preferentially directed to the cervical enlargement, strongly enhances the efficacy of M1 stimulation to evoke a contralateral forelimb motor response. This supports use of our neuromodulatory strategy to promote the motor cortical activity-based approach after injury.

3.4. Stimulation promotes forelimb movements after C4 contusion

We examined changes in performance on the horizontal ladder task and the IBB manipulation score to determine if combined tsDCS and iTBS for 10 days leads to improved motor function. Animals did not perform either task consistently until about 3 weeks post-injury. Week 3 is immediately after the stimulation period. Week 3 was the first test for the ladder task and week 4 was the first test for the IBB task. We reasoned that if stimulation promotes motor recovery, task performance should be more impaired on the first testing session (week 3 or 4) weeks and improved at 6 weeks. We compared performance at these two times. Horizontal ladder task performance and IBB scores before injury were not different for the two animal groups.

Fig. 4A–C plots changes in locomotor error rate for each animal in the study, presented for each limb separately (A, B) and total error (C). For the injury-only group, performance did not significantly improve between weeks 3 and 6, for either limb separately or for total error (left limb, 1.9% reduction in errors from week 3 to week 6; right limb, 2.6% reduction; total error, 2.6% reduction; paired *t*-tests for each limb and total errors: NS). To summarize for total errors of the injury-only group, the 2.6% reduction in total error rate corresponds to an overall 7% performance improvement between weeks 3 and 6, in relation to week 3, which was not significant. By contrast, we observed consistent overall improvement in the injury plus stimulation group. For the left limb all but one animal showed improvement (15.2% reduction; paired *t*-test: p = 0.002) and, for the right limb, all but 3 animals showed a reduction (8.2%; paired *t*-test: NS). For total error, 8 out of 9 injured plus stimulated animals showed a reduced error rate during the same period, so that the group overall performed significantly better (11.1% reduction; paired *t*-test: p = 0.003). To summarize for total errors of the injury plus stimulation group, the 11.1% reduction in total error rate corresponds to a significant overall 23% improvement in performance between weeks 3 and 6.

The IBB score is a bimanual measure of the expression of forepaw manipulation skills while eating two pieces of sweetened cereal (donut and spherical shapes). Normal performance receives a score of 9 (Fig. 4D). At 4 week there is no significant difference between groups. At week 6, the stimulated group performed significantly better than the injury-only group (injury: 5.43 ± 0.47; injury plus stimulation: 6.79 ± 0.0.31; unpaired *t*-test: p = 0.01). The insets show performance of individual animals in each group. On an individual animal basis, there was a significant improvement only in the stimulated group (injury-only: 5.05 ± 0.37 at week 4; 5.42 ± 0.47 at week 6; NS; injury plus stimulation: 5.77 ± 0.38 at week 4; 6.79 ± 0.31 at week 6; paired *t*-test; p = 0.009). Our findings show that combined tsDCS and iTBS for 10 days during the semi-acute period after C4 contusion injury leads to improved function in skilled locomotion and manipulation.

Author Manuscript Author Manuscript Author Manuscript Author Manuscript

3.5. Stimulation promotes CST outgrowth caudal to the lesion

After completion of the behavioral experiments, the CST was traced unilaterally and, 10 days later, animals were euthanized and spinal tissue was processed for BDA histochemistry. There was no difference in the number of spared CST axons in the white matter caudal to the C4 contusion in injury-only and injury plus stimulation groups (injury-only: 34.66 ± 6.32 axons; injury plus stimulation: 36.48 ± 5.07; $p = 0.83$). These values are similar to those reported in a prior study for moderate cervical contusion injury (Anderson et al., 2009). Average total axon length, corrected for tracer efficacy, was 12.5% higher in the injury plus stimulated group than the injury-only group (Injury-only: 11,728 ± 2561; Injury plus stimulation: 13,192 ± 2955; NS). We observed considerable variability between animals in each group.

A between group analysis does not take into account inter-animal differences in the number of spared axons descending to the segments caudal to the injury which is a major determinant for total outgrowth. To consider this important factor further, we next conducted a regression analysis where we compared the effect of total number of spared CST axons in the lateral and ventral white matter (bilaterally) caudal to the injury on two CST outcome measures, total gray matter axon length (Fig. 5A, B) and total varicosity number (Fig. 5C, D), also caudal to the injury. The slope of this relationship indicates the extent of gray matter CST axon length for each spared white matter axon for the cohort of animals. The difference in the slope of the regression lines estimates the effect that stimulation has on spared gray matter CST outgrowth. The slope of the relation in the injury plus stimulation group was significant and twice that of the injury-only group, which was not significant (Injury-only: slope = 0.21; $R = 0.45$, NS, $n = 12$; injury plus stimulation: slope = 0.49; $R = 0.88$, $n = 12$, $p < 0.01$). We conducted a similar analysis for axon varicosities, as a measure of putative presynaptic sites (see Methods section). Here too, there was an increase in the slope after stimulation and a significant relationship (Injury-only: 1.9, $R = 0.18$, NS; injury plus stimulation: 7.26, $R = 0.68$, $p < 0.01$). We constructed CST heat maps to show local axon length and axon varicosity density. To emphasize the relationship with spared white matter axons, we conducted a novel image-based analysis where we weighted each animal's contribution to the ensemble heat map by its number of spared axons (see Methods section). This representation shows an increase in the density of CST gray matter axons and varicosities. The overall topography remains similar in the injury-only and injury plus stimulation groups. Our findings suggest that combined spinal cord tsDCS and M1 iTBS stimulation for 10 days during the subacute period increased CST axons and connections (i.e., axon varicosities) below the injury.

3.6. Stimulation promotes CST outgrowth rostral to the lesion

We next determined if stimulation also increased outgrowth rostral to the injury. We examined the contralateral projections at C3 using the Space Balls stereological approach (see Methods section). The average total corrected axon length was 9.3% higher density of contralateral labeling in the injury plus stimulated group than the injury-only group (Injury: 165,301 ± 16,506; injury plus stimulation: 180,732 ± 15,413; $p = 0.51$).

Author Manuscript Author Manuscript Author Manuscript Author Manuscript

Similar to our analysis of spared caudal CST axons, we developed a metric of gray matter axon length per descending CST axon, which corresponds to an arithmetic transformation of the correction factor used to assay tracer efficacy (see Methods section). For this regression analysis we used the uncorrected CST axon length estimate for each animal and regressed these values against the each animal's estimate of the number of traced dorsal column axons. Each data point in Fig. 6 corresponds to the axon length-axon number ratio; the difference in the slope of the regression lines represent the effect that stimulation has on gray matter CST outgrowth. With stimulation we observed a 6.2-fold increase in slope (Injury-only: slope = 15.14; R = 0.208, n = 12, NS; injury plus stimulation: slope = 94.05; R = 0.772, n = 11, $p < 0.01$). Ensemble heat maps, based on individual animal data, shows that a similar increase in the central "hot spot" of projections. Thus, stimulation also promotes injury-dependent sprouting rostral to the injury.

4. Discussion

We show that a novel neuromodulatory approach is effective in significantly improving two skilled motor behaviors that depend on the corticospinal system for their control, horizontal ladder walking and manipulation. This recovery of skilled movement associates with CST sprouting below and above the level of a C4 contusion injury. The neuromodulatory approach that we used, which incorporates bilateral M1 iTBS stimulation and cathodal tsDCS, produces CST repair and partial recovery of skilled motor behaviors that, to perform well, requires the animals to integrate posture, external and internal sensory information, and intent.

4.1. Neuromodulatory approach to promoting axonal outgrowth

In intact animals and after pyramidal track lesion, M1 phasic stimulation produces a small motor response, which may be a small amplitude contralateral forelimb movement or an EMG response only. Because stimulation produces a motor response, it demonstrates the efficacy of the stimulation and ensures activation of the entire corticospinal motor circuit, which also includes indirect projections routed through the brain stem (Carmel et al., 2013). Recognizing the importance of pathway activation in promoting CST sprouting, our approach to activity-based CST repair across several models has been to adjust M1 stimulation to evoke a muscle response or movement (Brus-Ramer et al., 2007; Carmel et al., 2010; Salimi et al., 2008; Salimi and Martin, 2004). iTBS strongly activates muscle in rats, as our earlier study showed (Song et al., 2016) and by itself produces CST axonal outgrowth after unilateral pyramidal tract lesion (A Amer, unpublished observations). Compared with 6 h of daily multipulse stimulation for 10 days (Brus-Ramer et al., 2007), iTBS is at least as effective when delivered for only 27 min daily, for 10 days.

With the loss of most CST projections caudal to the injury, comes the reduced capacity for M1 stimulation to activate spinal motor circuits, much less muscle (Oudega and Perez, 2012). Using cathodal tsDCS remarkably enhances the M1-evoked response after SCI, as we show in this study. We have found that FEM modeling is critical in targeting tsDCS (Song et al., 2015). Since tsDCS alone tends not to produce an overt EMG response, a negative effect of this stimulation may be due to insufficient delivery of current to key levels of the cord.

Author Manuscript Author Manuscript Author Manuscript Author Manuscript

The mechanisms underlying spinal DC neuromodulation are not well-understood. Increased CST neurotransmitter release is suggested (Ahmed and Wieraszko, 2012), consistent with increased spinal CST-evoked synaptic responses (Song and Martin, 2017). Several studies recently have begun to elucidate localized electrophysiological changes that inform systems-level mechanisms. Jankowska and Bolzoni have shown that local DC stimulation can enhance the afferent group 1a-evoked motoneuron EPSP, as well as dorsal interneuronal responses (Bolzoni and Jankowska, 2015). Using a multielectrode recording array, we found that cathodal tsDCS preferentially enhances ventral depolarizing responses evoked by M1 stimulation, also suggesting an important motoneuronal locus for neuromodulatory effects (Song and Martin, 2017). Cathodal tsDCS enhances the H-reflex (Song et al., 2015), but generally has a more modest effect on spinal responses evoked by stimulation of large-diameter afferents than motor cortex stimulation (Song and Martin, 2017). Thus, whereas cathodal tsDCS likely enhances spinal cord excitability generally it has varied influences on different spinal systems. Whereas it is plausible that tsDCS alone contributes directly to repair and partial motor recovery, because of its capacity to modulate the spinal response of evoked cortical and peripheral stimulation, this needs to be tested directly.

4.2. CST repair after cervical SCI

The magnitude of the sprouting response caudal to the injury seemed less than what we have observed for stimulation-dependent sprouting after pyramidal tract lesion (Brus-Ramer et al., 2007; Song et al., 2016). This is likely due to the sparse numbers of spared axons caudal to the lesion in the present study. The dorsal CST was eliminated in all animals, injury-only and injury plus stimulation alike. Caudal to the injury, spared gray matter CST axons were essentially limited to the contralateral side. These axons derived predominantly from the contralateral lateral CST axons. Although we only labeled one side, M1 in both hemispheres was stimulated. We reason that a similar stimulation-induced sprouting response was present on the non-traced side.

Since the severity of the injury varied across animals, resulting in a range of spared CST axons at the enlargement level, it is not possible simply to compare total CST gray matter outgrowth in the two groups. The metric we used was to regress gray matter length with the number of spared white matter axons. Stimulation converted an insignificant relation in the injury-only group to one with a higher and significant slope. The slope represents gray matter axon length for each spared CST white matter axon. Not surprisingly, there was little or no relationship in the non-stimulated condition. Whereas stimulation drives outgrowth, we do not know the factors that contribute to axon length after injury-only.

We also examined CST changes rostral to the injury. Although this termination field of the CST is located rostral to the highest density territory for tsDCS, according to our FEM modeling, the need for tsDCS neuromodulation during the therapy period is less critical at a level where the CST is intact. We assayed the effect of stimulation on the CST by regressing gray matter axon length at C3 with an estimate of total CST dorsal column axon number. As with the CST results caudal to the injury, this regression showed significance in the injury plus stimulation group, along with a steeper slope than in the injury-only group. We interpret this finding as a predominant effect of stimulation on injured dorsal column CST axons,

Author Manuscript Author Manuscript Author Manuscript Author Manuscript

which make up the bulk of the projection to the contralateral gray matter. This is important because it suggests that axotomized CST neurons are able to mount an activity-dependent sprouting response. After axotomy, the ribosomal protein phospho-s6, which is used as a marker for mTOR activation, is down-regulated (Geoffroy et al., 2015; Liu et al., 2010). Since mTOR activation is necessary for CST axonal outgrowth after injury (Geoffroy et al., 2015; Liu et al., 2010; Park et al., 2008), mTOR downregulation is thought to limit the capacity for CST repair. Future experiments are necessary to determine the effect of M1 stimulation in mTOR activation.

Outgrowth rostral to the injury is also important as a potential avenue for repair. Propriospinal interneurons that receive CST input are located at this level and project to the enlargement segments via the ventral and ventrolateral spinal white matter columns (Alstermark et al., 2007; Azim et al., 2014). C3-level activity-dependent CST outgrowth may result in more connections between the CST and short propriospinal neurons that can, in turn, relay CST signals via spared white matter columns to segmental neurons caudal to the lesion. Injury-dependent sprouting of the CST on to propriospinal interneurons has been suggested as a mechanisms for recovery of hand function after C4/C5 lateral section in monkeys (Sasaki et al., 2004).

4.3. Combined stimulation improved skilled motor behavior after SCI

Stimulation led to significant improvement in both the IBB score and horizontal ladder walking. Improvement in ladder walking likely reflects M1 control signals that are better timed to each step and scaled to the locations of the ladder rungs after stimulation than to changes in the basic function of cervical pattern generators. For reaching and visually-guided stepping, upper cervical propriospinal neurons are thought to play a more important role than segmental interneurons (Alstermark et al., 1986; Alstermark and Kummel, 1986; Azim et al., 2014). Perhaps improvement in ladder walking reflects reorganization of C3 segmental circuits after stimulation-induced sprouting. Improved manipulation skills after injury, as revealed by significantly higher IBB scores in the stimulation group, may reflect segmental more than propriospinal control (Alstermark et al., 1986; Alstermark and Kummel, 1986), and CST sprouting within the enlargement segments. The rubrospinal tract is thought to mediate distal control together with the CST. Thus, as with M1 stimulation after pyramidal tract lesion, and the associated behavioral recovery (Carmel et al., 2010; Carmel et al., 2014; Song et al., 2016), changes in performance after SCI are apt to be mediated by multiple systems. Whereas we stimulate the corticospinal motor system, and have assayed that system anatomically and physiologically (Song et al., 2016; Song and Martin, 2017), it is likely that there are more complex and diverse activity-dependent changes in multiple systems.

4.4. Translation of M1 iTBS and tsDCS to the human

Both iTBS and tsDCS are well suited for implementation in humans. iTBS is routinely performed non-invasively using TMS (Huang et al., 2005). tsDCS is non-invasive and has been performed safely in human cervical spinal cord for modulating respiratory function (Niérat et al., 2014). A potential advantage of the “open loop” neuromodulatory approach used in this study is that it does not depend on the timing of critical neural events, such as

Author Manuscript Author Manuscript Author Manuscript Author Manuscript

with paired associative stimulation (Thickbroom, 2007), or on the occurrence of motor event, such as in “closed loop” stimulation paradigms (e.g., (McPherson et al., 2015)). It will be interesting in future experiments to determine if cortical or spinal stimulation delivered at particular times during the execution of a behavioral task results in an added benefit. However, a testament to the efficacy of the approach used is that we have observed improvement in motor function 5 weeks after beginning stimulation and CST sprouting at 7 weeks. An important question moving forward is what is the necessary dose to modulate cervical limb motor circuits in the human. Whereas this may be evaluated experimentally, FEM modeling is a way to scale stimulation parameters from the rat to the human. Whereas iTBS may be a potentially powerful way to provoke CST sprouting after injury, many questions remain unanswered, including optimizing the stimulation protocol in time, duration, and laterality. Importantly, the behavioral improvement we observed occurred without any applied course of rehabilitation. Although it is a common clinical practice, serious injury limits a person’s capacity to perform rehabilitation. Neuromodulation of the corticospinal motor system is a way to bring about persistent plasticity that potentially will make a seriously injured person’s rehabilitation program more effective.

Acknowledgments

NYS Department of Health Spinal Cord Injury Board (JHM: C30606GG; AA: C30860GG); NIH (JHM: 2R01NS064004); Craig H. Neilsen Foundation (JHM: 261214; NZ: 385743). We thank Xiuli Wu for histology and Helen Borges Delfino De Souza and Ahmed Aboseria for help with tissue segmentation of rat imaging data. The authors thank Dr. Henning Voss and the staff of the Citigroup Biomedical Imaging Center, Weill Cornell Medical College (New York, New York), for help with MRI and CT imaging.

References

Ahmed Z, Wieraszko A. Trans-spinal direct current enhances corticospinal output and stimulation-evoked release of glutamate analog, D-2,33H-aspartic acid. J Appl Physiol. 2012; 112(9):1576–1592. [PubMed: 22362399]

Alstermark B, Kummel H. Transneuronal labelling of neurons projecting to forelimb motoneurons in cats performing different movements. Brain Res. 1986; 376:387–391. [PubMed: 3730842]

Alstermark B, Gorska T, Johannisson T, Lundberg A. Effects of dorsal column transection in the upper cervical segments on visually guided forelimb movements. Neurosci Res. 1986; 3:462–466. [PubMed: 3748476]

Alstermark B, Isa T, Pettersson LG, Sasaki S. The C3–C4 propriospinal system in the cat and monkey: a spinal pre-motoneuronal centre for voluntary motor control. Acta Physiol (Oxford). 2007; 189:123–140.

Anderson KD. Targeting recovery: priorities of the spinal cord-injured population. J Neurotrauma. 2004; 21:1371–1383. [PubMed: 15672628]

Anderson DK, Beattie M, Blesch A, Bresnahan J, Bunge M, Dietrich D, Dietz V, Dobkin B, Fawcett J, Fehlings M, Fischer I, Grossman R, Guest J, Hagg T, Hall ED, Houle J, Kleitman N, McDonald J, Murray M, Privat A, Reier P, Steeves J, Steward O, Tetzlaff W, Tuszynski MH, Waxman SG, Whittemore S, Wolpaw J, Young W, Zheng B. Recommended guidelines for studies of human subjects with spinal cord injury. Spinal Cord. 2005; 43:453–458. [PubMed: 15824756]

Anderson KD, Sharp KG, Steward O. Bilateral cervical contusion spinal cord injury in rats. Exp Neurol. 2009; 220:9–22. [PubMed: 19559699]

Azim E, Jiang J, Alstermark B, Jessell TM. Skilled reaching relies on a V2a propriospinal internal copy circuit. Nature. 2014; 508:357–363. [PubMed: 24487617]

Author Manuscript Author Manuscript Author Manuscript Author Manuscript

Benali A, Trippe J, Weiler E, Mix A, Petrasch-Parwez E, Girzalsky W, Eysel UT, Erdmann R, Funke K. Theta-burst transcranial magnetic stimulation alters cortical inhibition. J Neurosci. 2011; 31:1193–1203. [PubMed: 21273404]

Benowitz LI, He Z, Goldberg JL. Reaching the brain: advances in optic nerve regeneration. Exp Neurol. 2017; 287:365–373. [PubMed: 26746987]

Bolzoni F, Jankowska E. Presynaptic and postsynaptic effects of local cathodal DC polarization within the spinal cord in anaesthetized animal preparations. J Physiol. 2015; 593:947–966. [PubMed: 25416625]

Brus-Ramer M, Carmel JB, Chakrabarty S, Martin JH. Electrical stimulation of spared corticospinal axons augments connections with ipsilateral spinal motor circuits after injury. J Neurosci. 2007; 27:13793–13801. [PubMed: 18077691]

Carmel JB, Berrol LJ, Brus-Ramer M, Martin JH. Chronic electrical stimulation of the intact corticospinal system after unilateral injury restores skilled locomotor control and promotes spinal axon outgrowth. J Neurosci. 2010; 30:10918–10926. [PubMed: 20702720]

Carmel JB, Kimura H, Berrol LJ, Martin JH. Motor cortex electrical stimulation promotes axon outgrowth to brain stem and spinal targets that control the forelimb impaired by unilateral corticospinal injury. Eur J Neurosci. 2013; 37:1090–1102. [PubMed: 23360401]

Carmel JB, Kimura H, Martin JH. Electrical stimulation of motor cortex in the uninjured hemisphere after chronic unilateral injury promotes recovery of skilled locomotion through ipsilateral control. J Neurosci. 2014; 34:462–466. [PubMed: 24403146]

Chen Y, He Y, DeVivo MJ. Changing demographics and injury profile of new traumatic spinal cord injuries in the United States, 1972–2014. Arch Phys Med Rehabil. 2016; 97:1610–1619. [PubMed: 27109331]

Friel K, Martin JH. Bilateral activity-dependent interactions in the developing corticospinal system. J Neurosci. 2007; 27:11083–11090. [PubMed: 17928450]

Friel K, Chakrabarty S, Kuo HC, Martin J. Using motor behavior during an early critical period to restore skilled limb movement after damage to the corticospinal system during development. J Neurosci. 2012; 32:9265–9276. [PubMed: 22764234]

Gabriel S, Lau RW, Gabriel C. The dielectric properties of biological tissues: II. Measurements in the frequency range 10 Hz to 20 GHz. Phys Med Biol. 1996; 41:2251–2269. [PubMed: 8938025]

Geoffroy CG, Lorenzana AO, Kwan JP, Lin K, Ghassemi O, Ma A, Xu N, Creger D, Liu K, He Z, Zheng B. Effects of PTEN and Nogo codeletion on corticospinal axon sprouting and regeneration in mice. J Neurosci. 2015; 35:6413–6428. [PubMed: 25904793]

Hernandez-Labrado GR, Polo JL, Lopez-Dolado E, Collazos-Castro JE. Spinal cord direct current stimulation: finite element analysis of the electric field and current density. Med Biol Eng Comput. 2011; 49:417–429. [PubMed: 21409426]

Huang YZ, Edwards MJ, Rounis E, Bhatia KP, Rothwell JC. Theta burst stimulation of the human motor cortex. Neuron. 2005; 45:201–206. [PubMed: 15664172]

Huang Y, Liu AA, Lafon B, Friedman D, Dayan M, Wang X, Bikson M, Doyle WK, Devinsky O, Parra LC. Measurements and models of electric fields in the in vivo human brain during transcranial electric stimulation. elife. 2017:6.

Irvine KA, Ferguson AR, Mitchell KD, Beattie SB, Beattie MS, Bresnahan JC. A novel method for assessing proximal and distal forelimb function in the rat: the Irvine, Beatties and Bresnahan (IBB) forelimb scale. J Vis Exp. 2010

Irvine KA, Ferguson AR, Mitchell KD, Beattie SB, Lin A, Stuck ED, Huie JR, Nielson JL, Talbott JF, Inoue T, Beattie MS, Bresnahan JC. The Irvine, Beatties, and Bresnahan (IBB) forelimb recovery scale: an assessment of reliability and validity. Front Neurol. 2014; 5:116. [PubMed: 25071704]

Liu K, Lu Y, Lee JK, Samara R, Willenberg R, Sears-Kraxberger I, Tedeschi A, Park KK, Jin D, Cai B, Xu B, Connolly L, Steward O, Zheng B, He Z. PTEN deletion enhances the regenerative ability of adult corticospinal neurons. Nat Neurosci. 2010; 13:1075–1081. [PubMed: 20694004]

Maier IC, Baumann K, Thallmair M, Weinmann O, Scholl J, Schwab ME. Constraint-induced movement therapy in the adult rat after unilateral corticospinal tract injury. J Neurosci. 2008; 28:9386–9403. [PubMed: 18799672]

Author Manuscript Author Manuscript Author Manuscript Author Manuscript

Martin JH, Kably B, Hacking A. Activity-dependent development of cortical axon terminations in the spinal cord and brain stem. Exp Brain Res. 1999; 125:184–199. [PubMed: 10204771]

McPherson JG, Miller RR, Perlmutter SI. Targeted, activity-dependent spinal stimulation produces long-lasting motor recovery in chronic cervical spinal cord injury. Proc Natl Acad Sci U S A. 2015; 112:12193–12198. [PubMed: 26371306]

Meng Z, Li Q, Martin JH. The transition from development to motor control function in the corticospinal system. J Neurosci. 2004; 24:605–614. [PubMed: 14736845]

Metz GA, Whishaw IQ. Cortical and subcortical lesions impair skilled walking in the ladder rung walking test: a new task to evaluate fore- and hindlimb stepping, placing, and co-ordination. J Neurosci Methods. 2002; 115:169–179. [PubMed: 11992668]

Mouton PR, Long JM, Lei DL, Howard V, Jucker M, Calhoun ME, Ingram DK. Age and gender effects on microglia and astrocyte numbers in brains of mice. Brain Res. 2002; 956:30–35. [PubMed: 12426043]

Niérat MC, Similowski T, Lamy JC. Does trans-spinal direct current stimulation alter phrenic motoneurons and respiratory neuromechanical outputs in humans? A double-blind, sham-controlled, randomized, crossover study. J Neurosci. 2014; 34:14420–14429. [PubMed: 25339753]

NSCISC. Spinal cord injury facts and figures at a glance. J Spinal Cord Med. 2014; 37:659–660. [PubMed: 25229744]

Oudega M, Perez MA. Corticospinal reorganization after spinal cord injury. J Physiol. 2012; 590:3647–3663. [PubMed: 22586214]

Park KK, Liu K, Hu Y, Smith PD, Wang C, Cai B, Xu B, Connolly L, Kramvis I, Sahin M, He Z. Promoting axon regeneration in the adult CNS by modulation of the PTEN/mTOR pathway. Science. 2008; 322:963–966. [PubMed: 18988856]

Park KK, Liu K, Hu Y, Kanter JL, He Z. PTEN/mTOR and axon regeneration. Exp Neurol. 2010; 223:45–50. [PubMed: 20079353]

Rahman A, Reato D, Arlotti M, Gasca F, Datta A, Parra LC, Bikson M. Cellular effects of acute direct current stimulation: somatic and synaptic terminal effects. J Physiol. 2013; 591:2563–2578. [PubMed: 23478132]

Salimi I, Martin JH. Rescuing transient corticospinal terminations and promoting growth with corticospinal stimulation in kittens. J Neurosci. 2004; 24:4952–4961. [PubMed: 15163687]

Salimi I, Friel KM, Martin JH. Pyramidal tract stimulation restores normal corticospinal tract connections and visuomotor skill after early postnatal motor cortex activity blockade. J Neurosci. 2008; 28:7426–7434. [PubMed: 18632946]

Sasaki S, Isa T, Pettersson LG, Alstermark B, Naito K, Yoshimura K, Seki K, Ohki Y. Dexterous finger movements in primate without monosynaptic corticomotoneuronal excitation. J Neurophysiol. 2004; 92:3142–3147. [PubMed: 15175371]

Scheff SW, Rabchevsky AG, Fugaccia I, Main JA, Lumpp JE Jr. Experimental modeling of spinal cord injury: characterization of a force-defined injury device. J Neurotrauma. 2003; 20:179–193. [PubMed: 12675971]

Sharif-Alhoseini M, Khormali M, Rezaei M, Safdarian M, Hajighadery A, Khalatbari MM, Safdarian M, Meknatkhah S, Rezvan M, Chalangari M, Derakhshan P, Rahimi-Movaghar V. Animal models of spinal cord injury: a systematic review. Spinal Cord Adv (online publication). 2017

Song W, Martin JH. Spinal cord direct current stimulation differentially modulates neuronal activity in the dorsal and ventral spinal cord. J Neurophysiol. 2017; 117:1143–1155. [PubMed: 28031400]

Song W, Truong DQ, Bikson M, Martin JH. Transspinal direct current stimulation immediately modifies motor cortex sensorimotor maps. J Neurophysiol. 2015; 113:2801–2811. [PubMed: 25673738]

Song W, Amer A, Ryan D, Martin JH. Combined motor cortex and spinal cord neuromodulation promotes corticospinal system functional and structural plasticity and motor function after injury. Exp Neurol. 2016; 277:46–57. [PubMed: 26708732]

Thickbroom GW. Transcranial magnetic stimulation and synaptic plasticity: experimental framework and human models. Exp Brain Res. 2007; 180:583–593. [PubMed: 17562028]

Toshev PK, Guleyupoglu B, Bikson M. Informing dose design by modeling transcutaneous spinal direct current stimulation. Clin Neurophysiol. 2014

Author Manuscript Author Manuscript Author Manuscript Author Manuscript

Wagner T, Fregni F, Fecteau S, Grodzinsky A, Zahn M, Pascual-Leone A. Transcranial direct current stimulation: a computer-based human model study. NeuroImage. 2007; 35:1113–1124. [PubMed: 17337213]

Author Manuscript Author Manuscript Author Manuscript Author Manuscript

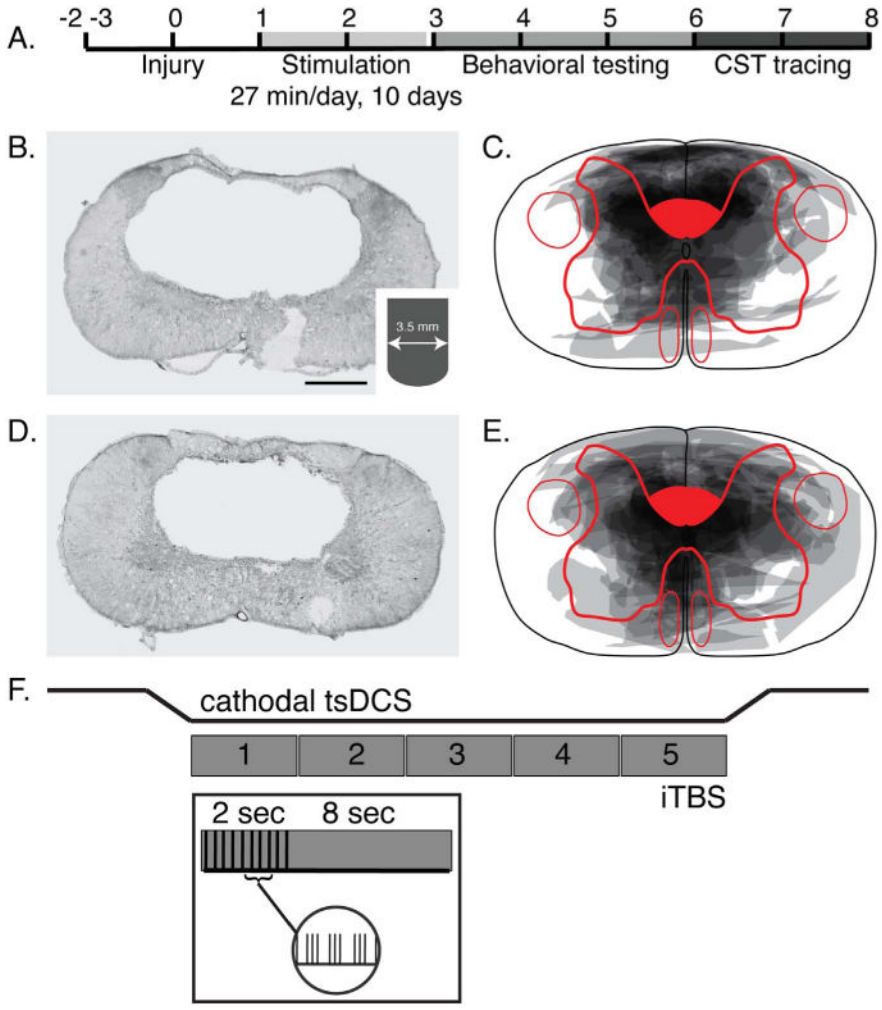

Fig. 1.

Methods employed in the study. A. Time-line for experiments. At approximately 2–3 weeks before injury animals received cortical epidural electrode implantation and initial training in the ladder and IBB tasks. B, D. Representative lesion in injury-only (B) and injury plus stimulation (D) animals. Overlay plots show lesion extent across animals (C, E). The darker the region, the greater the amount of overlap between animals. Calibration (B): 500 μm. Inset in B shows the configuration of the tip of the impactor probe. F. Stimulation paradigm.

Author Manuscript Author Manuscript Author Manuscript Author Manuscript

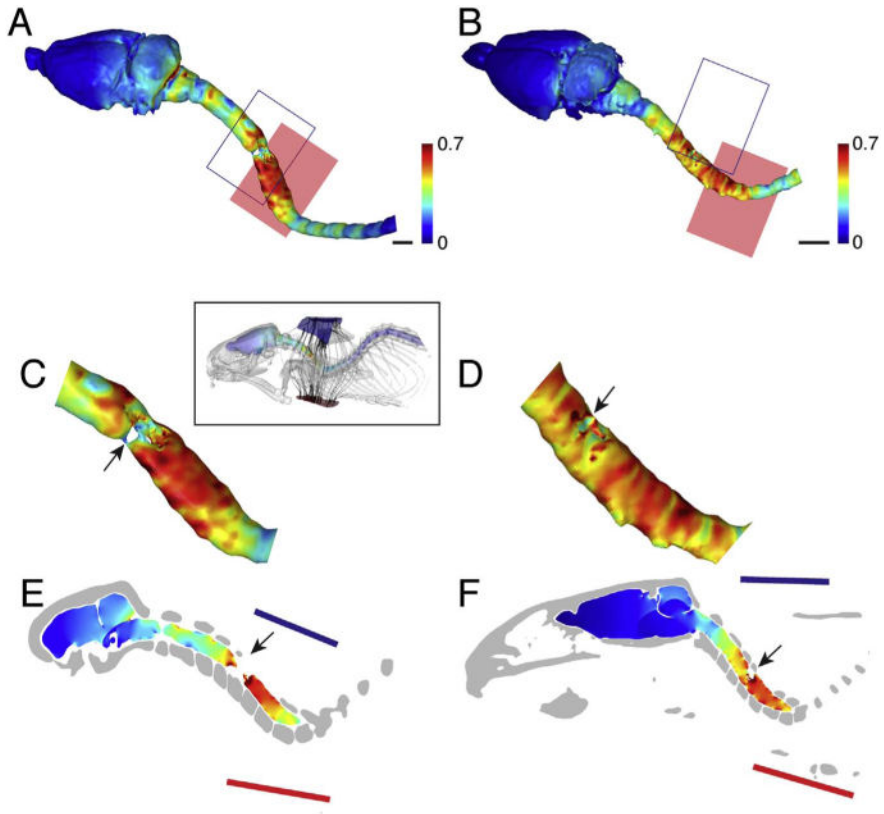

Fig. 2.

Finite Element Method modeling of current density. Representation of current flow is depicted in the inset below part A. The cathode is located dorsally and the anode, ventrally. A–F. Data from two animals (left and right columns) in which FEM modeling was performed. Surface views (A, B), expanded region of lesion (C, D), and view approximately at the midline (E, F). Current density is represented according to a color scale. The cathode is represented by the blue rectangle and the anode, by the pink rectangle. Color scale same for all images; max = 0.7 A/m^2. Length: 5 mm. (For interpretation of the references to color in this figure legend, the reader is referred to the web version of this article.)

Author Manuscript Author Manuscript Author Manuscript Author Manuscript

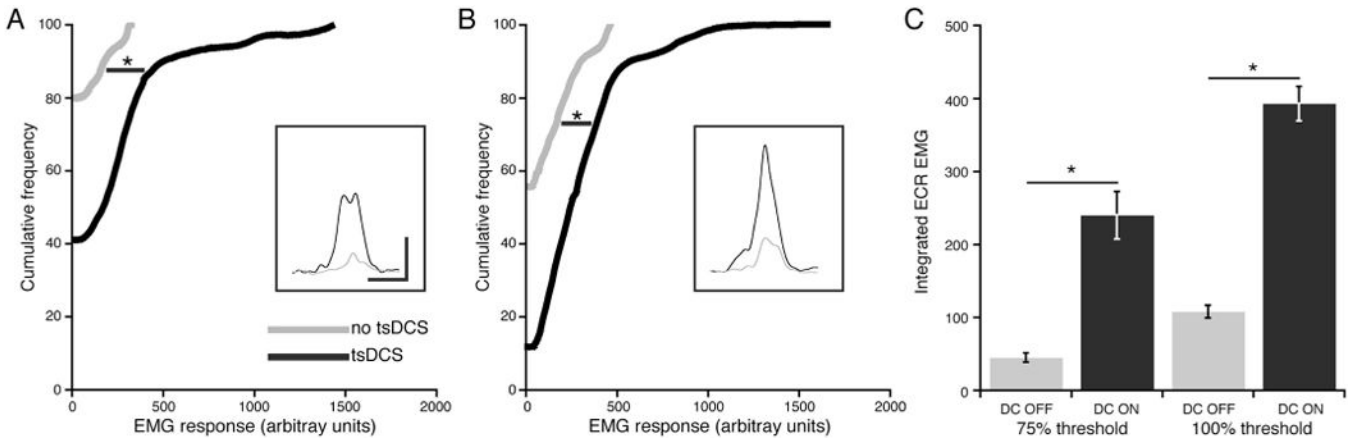

Fig. 3.

tsDCS modulation of MEPs at 75–85% (A) and 100% (B) movement threshold. Cumulative distribution histograms without tsDCS (gray) and with tsDCS (black). The cumulative distribution histograms were smoothed using a Stineman function (KaliedaGraph). Insets show representative average MEP. C. Graphs plotting mean ± SE of EMG responses for 75–85% (left pair) and 100% (right pair) threshold. Values obtained without tsDCS are shown in gray and during tsDCS, in black. N = 3 animals. Calibrations (inset part A; apply to both A and B): 0.01 mV, 5 ms.

Author Manuscript Author Manuscript Author Manuscript Author Manuscript

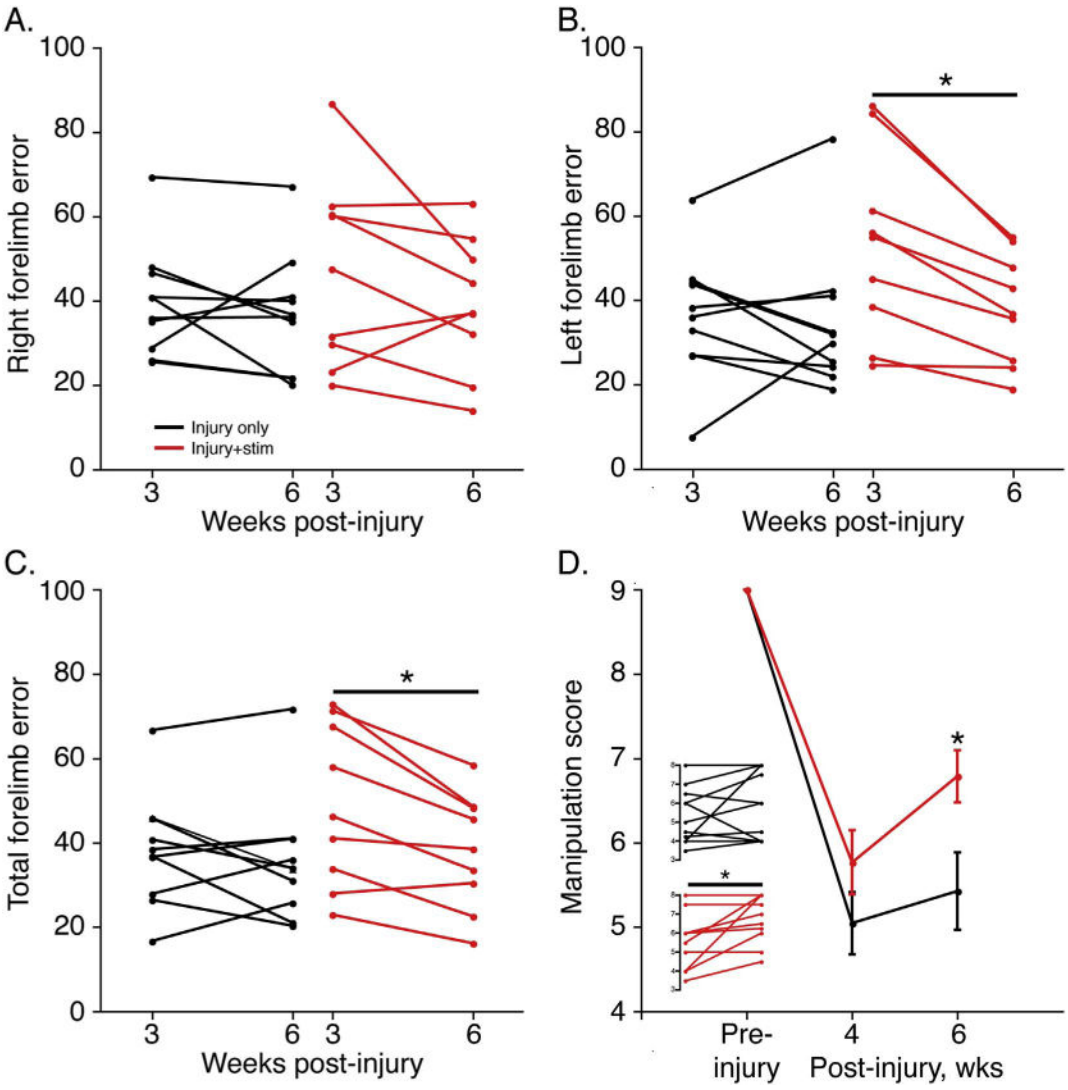

Fig. 4.

Effect of stimulation on motor performance. Black lines plot data for injury only animals; red lines, for injury + stimulation. A, B, C. Performance errors in the horizontal ladder task for the right forelimb (A), left forelimb (B; injury + stimulation, paired *t*-test; p = 0.002) and average total error (C, injury + stimulation, paired *t*-test; p = 0.003). D. IBB performance. Group average (injury plus stimulation; unpaired *t*-test; p = 0.01). Inset show data for individual animals for the injury-only group (black; paired *t*-test, NS) and the injury plus stimulation group (red; paired *t*-test, p = 0.009). (For interpretation of the references to color in this figure legend, the reader is referred to the web version of this article.)

Author Manuscript Author Manuscript Author Manuscript Author Manuscript

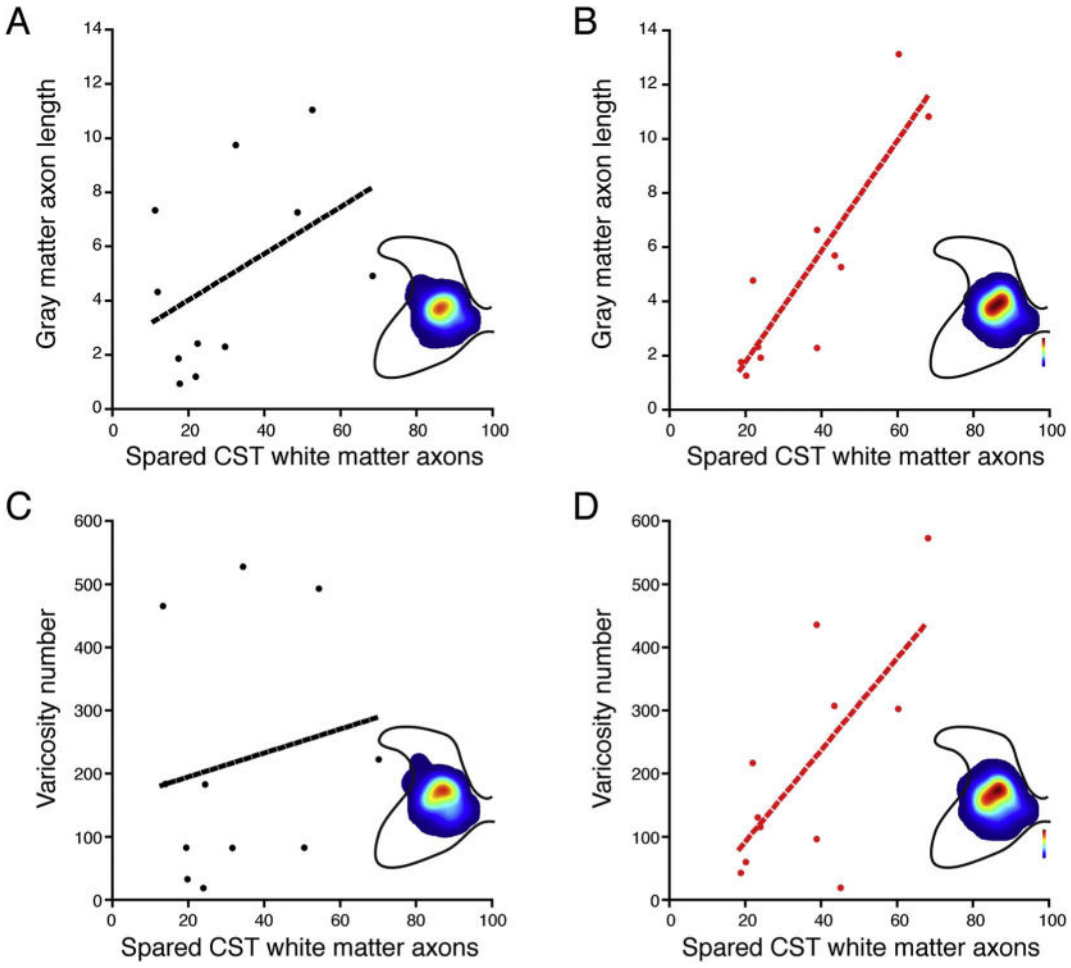

Fig. 5.

Relationship between gray matter axon length (A, B) and varicosities (C, D) and the number of spared white matter axons for each animal caudal to the injury. Left column (A, C) plot data for injury-only animals (n = 12), and right column (B, D) plot data for the injury plus stimulation group (n = 11). The slopes and R values for each graph are: A. Axon length, injury-only. Slope = 0.208; R = 0.45; NS. B. Axon length, injury plus stimulation. Slope = 0.492; R = 0.88, $p < 0.05$. C. Varicosity number, injury-only. Slope = 1.9, R-0.18, NS. D. Varicosity number, injury plus stimulation. Slope = 7.27, R = 0.68; $p < 0.05$. Inset show heat maps of CST axon (A, B) and CST varicosity (C, D) density. Color scale maximal value for axon length in A and B is 0.68. Color scale maximal value for varicosities in C and D is 0.075. (For interpretation of the references to color in this figure legend, the reader is referred to the web version of this article.)

Author Manuscript Author Manuscript Author Manuscript Author Manuscript

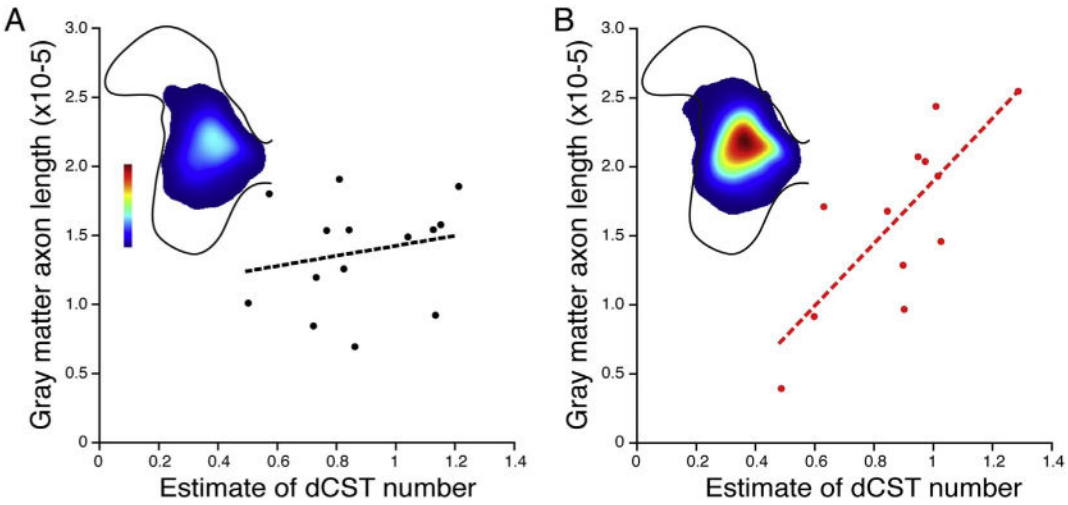

Fig. 6.

Relationship between gray matter axon length and the number of spared white matter axons for each animal for injury-only (A; n = 14) and injury plus stimulation (B; n = 13) rostral to the injury. Y-axis plots the average gray matter axon length measure in the C3 gray matter. The slopes and R values for each graph are: A. Axon length, injury-only. Slope = 15.14; R = 0.209; NS. B. Axon length, injury plus stimulation. Slope = 97.04; R = 0.77; $p < 0.05$. Color scale maximal value for axon length in A and B is 0.035 (arbitrary units). (For interpretation of the references to color in this figure legend, the reader is referred to the web version of this article.)